



RESEARCH ARTICLE

OPEN ACCESS

Bioactive Flavonoid used as a Stabilizing Agent of Mono and Bimetallic Nanomaterials for Multifunctional Activities

Noushad Karuvantevida¹ , Muthusamy Razia² , Ramalingam Bhuvaneshwar¹ , Gnanasekar Sathishkumar¹ , Seetharaman Prabukumar¹  and Sivaperumal Sivaramakrishnan^{1*} 

¹Department of Biotechnology, Bharathidasan University, Tiruchirappalli - 620 024, Tamilnadu, India.

²Department of Biotechnology, Mother Teresa Women's University, Kodaikanal - 624-101, Tamilnadu, India.

Abstract

The multifunctional features of noble metal nanoparticles (MNPs) were exploited in various biomedical applications, which eventually demanded the development of a sustainable green synthesis approach. In the present study, Quercetin (Q) was employed as a promising green reductant for the generation of noble metal nanoparticles such as silver (Q-AgNPs), gold (Q-AuNPs), and bimetallic (Q-Ag-AuNPs) towards biomedical perspective. Initially, the NPs were successfully synthesized in a size-controlled manner via optimizing temperature, pH, metal ion concentration, and stoichiometric ratio of the reaction mix. The redox reaction and conversion of metal ions (Ag^+ and Au^{3+}) into their respective metal nano-forms were confirmed through their surface plasmonic resonance (SPR) in UV-visible spectroscopy. In addition, different instrumentation like FT-IR, XRD, HR-TEM, and XPS analyses were performed to confirm the size, shape, and chemical composition of fabricated NPs. The bactericidal effect of fabricated NPs was tested against Gram-positive and Gram-negative pathogens. Moreover, the cytotoxic potential was screened against breast (MCF-7) and colorectal (HCT-116) carcinoma cell lines. This work revealed that the flavonoid-functionalized noble metal NPs were associated with good antibacterial and anticancer potential against selected cancer cell lines.

Keywords: Quercetin, Silver Nanoparticles, Bi-metallic, Green Synthesis, Antibacterial, Breast Carcinoma

*Correspondence: sivaramakrishnan123@gmail.com

Citation: Karuvantevida N, Razia M, Bhuvaneshwar R, Sathishkumar G, Prabukumar S, Sivaramakrishnan S. Bioactive Flavonoid used as a Stabilizing Agent of Mono and Bimetallic Nanomaterials for Multifunctional Activities. *J Pure Appl Microbiol.* 2022 ;16(3):1652-1662. doi: 10.22207/JPAM.16.3.03

© The Author(s) 2022. **Open Access.** This article is distributed under the terms of the [Creative Commons Attribution 4.0 International License](https://creativecommons.org/licenses/by/4.0/) which permits unrestricted use, sharing, distribution, and reproduction in any medium, provided you give appropriate credit to the original author(s) and the source, provide a link to the Creative Commons license, and indicate if changes were made.

INTRODUCTION

Due to the persistence and emergence of multidrug resistance (MDR), many new treatment alternatives are mandatory in combating infectious diseases.¹ On the other hand, the current chemotherapeutic options to cure various cancers face limitations like indiscriminate cytotoxicity and MDR-associated cancer stem cells (CSCs) growth. The conventional drugs in chemotherapy are hampered by the restricted accessibility of the drug to reach malignant tissues, which necessitates a higher dosage, resulting in adverse side effects and nonspecific targeting.² Nanomaterials-based therapeutic ventures are considered one of the fast-growing innovative technologies for improving earlier cancer diagnosis and treatment to sort out these limitations. Nanoscience is an interdisciplinary research area that mainly entails designing and fabricating materials (≤ 100 nm) with unique physiochemical features compared to their macroscale counterparts. For instance, the nanoparticles of noble metals with unique optical, electrical, and mechanical properties have widespread usage in many industrial, electronic, and healthcare products.³

Among the metal nanoparticles (MNPs), gold (AuNPs) and silver (AgNPs) were largely explored for biomedical-oriented applications due to their unique size, shape, and tunable surface properties.⁴ These two MNPs also have other benefits, such as intrinsic bioactivities, photo-absorbing capability, and intriguing optical characteristics. It was now well-established that the MNPs can easily pass through the cellular barriers and effectively internalize through leaky vasculature in a passive targeting mode.⁵ Based on this phenomenon, the fabricated Ag and AuNPs have been employed in antimicrobial, drug delivery, phototherapy, biosensing, imaging, and theranostic applications.⁶ The use of potentially harmful agents, low material conversion, and energy requirements persist in traditional physical and chemical methods of NPs fabrication.⁷ Although, the exploitation of various bio entities such as plants, microbes, actinomycetes, yeast, and other biowastes was an alternative eco-friendlier approach. The formation of polydispersed NPs, unclear reduction mechanism, and requirement of

multiple purification steps to eliminate impurities limits their applicability in a scaled-up industrial production.⁸ Therefore, there is a growing need to develop a single biomolecule-assisted sustainable NPs synthesis route for improved bio-applications.

Flavonoids are ubiquitous in plant extracts and encompass various functional properties such as physical, chemical, and biological effects. Thus, polyphenols have long been used in traditional medicine and diverse industrial applications. Nowadays, active polyphenols have been exploited to prepare functional materials mainly because of their biological activities and adhesive properties. Polyphenols interact with various nanoparticulate systems via hydrogen bonding, covalent bonding, metal coordination, hydrophobic, and electrostatic interactions due to their active functional groups.^{9,10} Therefore, polyphenols are widely compatible structural motifs for engineering materials for targeted applications spanning chemistry, materials science, and nanomedicine. After the booming research investigations on plant 'nanofactories' demonstrated that the phytoconstituents such as phenols, flavonoids, polysaccharides, and proteins contribute to various NPs generation.¹¹ Especially, the bioactive flavonoids play a dual role as an active reducing agent and stabilizer, which provide a thin layer of functional coating on fabricated NMs. In addition, the complexation of flavonoids with metallic ions ultimately enhances their solubility and bioavailability, which also minimizes their adverse side effects. It was reported that the hydroxyl group on the C₃ or C₅ position of a flavonoid aids in the formation of metal complexes. Most of the studies demonstrated that the biological activities of a specific flavonoid were improved after developing a coordination linkage with metallic ions.¹²

Amyriad of flavonoids has been screened for their therapeutic abilities to treat various ailments. Quercetin (3,3',4',5,7-pentahydroxyflavone) is an important flavonoid that possesses antioxidant, antimetastatic, anticancer, anti-inflammatory, and antidiabetic antiulcer properties.¹³ Interestingly, this active flavonoid triggers anticancer effects via G1/S transition or G2/M cell cycle arrest and hinders various molecular cascades' activity. However, the usage of Quercetin was limited in the

clinical translation due to its poor bioavailability and solubility.¹³⁻¹⁵ Hence, the bioactivities of Q-stabilized highly-stable metal nanoparticles such as silver, gold, and bi-metallic were tested to develop a bio-nano colloidal formulation for medical applications.

MATERIALS AND METHODS

Materials

Quercetin (C₁₅H₁₀O₇, MW: 302.24 g/mol) was obtained from Sigma-Aldrich (St. Louis, USA). Silver nitrate (AgNO₃, MW: 169.87 g/mol), Chloroauric acid (HAuCl₄, MW: 339.785 g/mol), and other chemicals were purchased from Himedia Mumbai Pvt. Ltd. Double distilled water was used in all experiments, the glassware was cleaned with running tap water followed by acetone rinsing and dried thoroughly in a hot air oven.

Synthesis of Q-Ag, Au, and Ag-AuNPs

Initially, the reaction mixture was prepared by adding 0.015g of Quercetin in 100ml of 1mM AgNO₃ solution separately under constant stirring at room temperature. Different reaction conditions such as temperature (37° C-100° C), pH-(6-10), the concentration of metal ion AgNO₃ & HAuCl₄ (0.5-3 mM), and stoichiometric proportion (1:1- 2:1) of the reaction mixture and incubation time (0-60 min) were fixed to control the nucleation and growth of NPs with better size distribution. Effects of these parameters on controlling the size, shape, and distribution of NPs were studied through the surface plasmon resonance (SPR) absorbance spectra in a UV-Visible spectrophotometer.

Instrumentation

Firstly, the generation of Q-Ag, Au, and Ag-AuNPs was confirmed with SPR peak observation

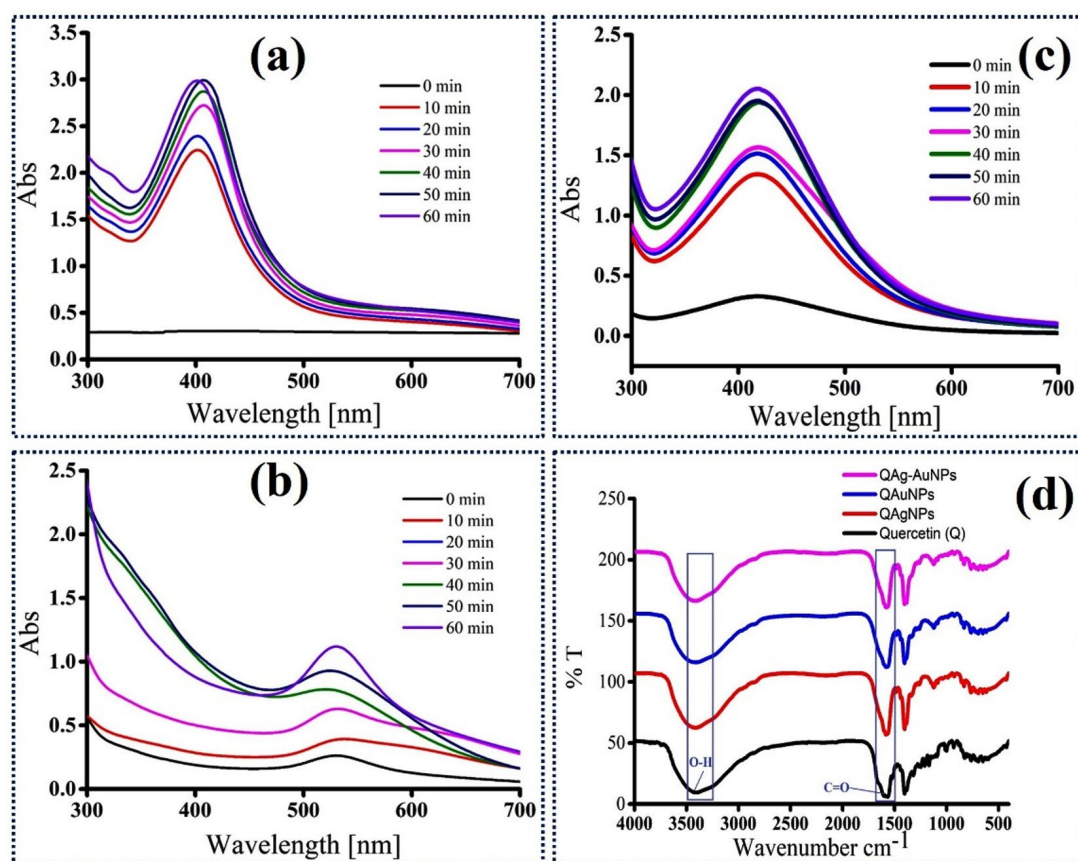


Figure 1. UV-Visible spectroscopic measurements of (a) Q-AgNPs, (b) Q-AuNPs, (c) Q-Ag-AuNPs, (d) FT-IR transmittance of pure Quercetin and fabricated nanomaterials.

in UV-Visible spectroscopic (JASCOV-650) analysis at 300–700 nm. Then, the hydrodynamic diameter, dispersity, and colloidal stability of fabricated NPs were measured using Malvern Zetasizer, Nano-ZS90 DLS, and ζ -potential analyzer. To Fig. out the plausible reduction mechanism, the FT-IR analysis was performed to elucidate the active functional groups of pure-Q responsible for reducing and stabilizing NPs. Briefly, the samples (pure-Q, Q-AgNPs, Q-AuNPs, and Q-Ag-AuNPs) were pelletized using KBr powder and recorded using JASCO 460 PLUS FTIR spectrometer (wavelength range between 4000 cm^{-1} to 500 cm^{-1}). To determine the dimension of synthesized NPs with h, k, l values and crystallinity type of NPs, the XRD pattern was recorded in PAN analytical X pert PRO Model. The HR-TEM micrographs, EDAX spectrum, and SAED pattern were recorded at various magnification ranges in JEOL JEM 2100 HR-TEM (100Kev).

In vitro Antibacterial Activity

Bacterial Cultures

Bacterial pathogens such as *Klebsiella*

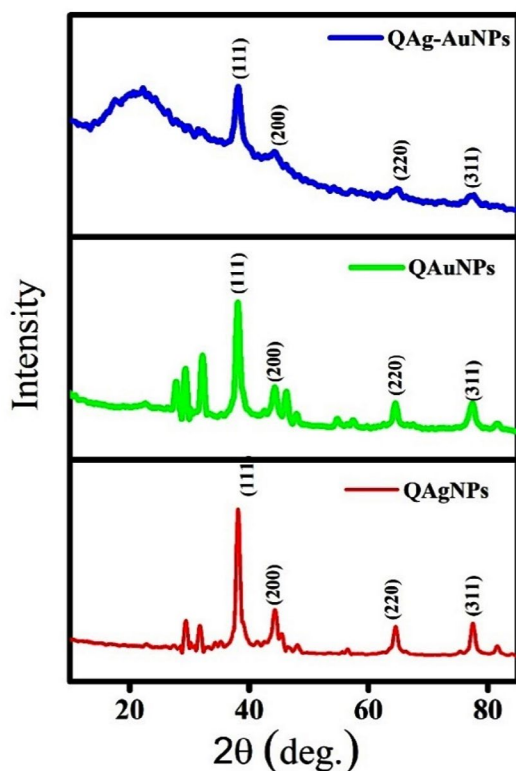


Figure 2. XRD spectrum of fabricated NPs.

pneumoniae (MTCC 530), *Escherichia coli* (MTCC 1687), *Vibrio cholera* (MTCC 0139), *Pseudomonas* (MTCC 512), *Proteus vulgaris* (MTCC 426), *Shigella dysenteriae* (ATCC 13313), *Streptococcus aureus* (MTCC 121), *Streptococcus pneumoniae* (MTCC 7465), *Bacillus* sp. (MTCC 511), *Bacillus Megaterium* (MTCC 5981) were collected from the Microbial Type Culture and Collection (MTCC) in Chandigarh, India.

Well Diffusion Assay

The antibacterial potential of fabricated NPs was comparatively studied using a well diffusion assay.¹⁷ All the bacterial pathogens were cultured in the Mueller-Hinton (M-H) broth at 37°C and then sub-cultured in M-H agar overnight. Then, the bacterial colonies were suspended in 2 mL of sterile saline, and the inoculum of test pathogens was prepared by adjusting the turbidity of bacterial suspensions to 0.5 McFarland (1.5×10^6 colony forming units CFU/mL) by diluting the sterile saline. All the bacterial pathogens inoculum was uniformly swabbed onto Mueller-Hinton (M-H) agar plates separately using sterilized cotton swabs. Meanwhile, the samples- 25 $\mu\text{g/mL}$ of streptomycin sulfate (PC), pure-Q, Q-AgNPs, Q-AuNPs and Q-Ag-AuNPs were loaded into each well. After overnight incubation at $37^{\circ}\text{C} \pm 0.2^{\circ}\text{C}$, the formation of clear zones around the well was measured with a zone scale.

In vitro Anticancer Studies

Cell Lines

MCF-7 human breast cancer cells and HCT-116 colorectal carcinoma cells were procured from American Type Culture Collection (ATCC). The cells were grown in a DMEM medium supplemented with 10% FBS. The antibiotics streptomycin and penicillin were added to the medium (both 100 U/mL, Sigma Chemical Co., St. Louis, MO, USA). In a Thermo Scientific (USA) incubator, the cells were incubated at 37°C in a humidified atmosphere with 5% CO_2 .

MTT Assay

The cytotoxicity effect of fabricated Q-AgNPs, Q-AuNPs, and Q-Ag-AuNPs was measured using MTT (3-(4,5-dimethylthiazol-2-yl)-2,5-diphenyl tetrazolium bromide) assay.¹⁸

Briefly, the breast (MCF-7) and colorectal (HCT-116) carcinoma cells were seeded at a density of 1×10^4 cells per well in 100 μ L of complete culture medium (DMEM or RPMI-1640) for the respective cell lines. After 24 hours, the medium was changed with 100 μ L of fresh incomplete medium containing different concentrations (1.56 to 100 μ g/mL) of samples and incubated for 48 h at 37°C in 5% CO₂. A fresh medium containing 0.40 mg mL⁻¹ MTT was added to the 96-well plates after the incubation period, and they were incubated for another 4 hours at 37°C in 5% CO₂. Then, the suspended NPs were separated by centrifuging at 20,000 rpm for 15 minutes and collecting the supernatant. After aspirating the medium, the formazan crystals generated after 4 hours were solubilized in 100 mL of DMSO. A 96-well plate reader was used to detect the absorbance at 595 nm (Bio-Rad, Hercules, CA, USA). The growth

inhibition was calculated using the following formula:

$$\% \text{ Cell viability} = \frac{\text{sample O.D.}}{\text{control O.D.}} \times 100$$

RESULTS AND DISCUSSION

Generally, the natural polyphenols obtained from the plant entities possess tremendous potential to reduce metal ions (Ag⁺ or Au³⁺) and act as a capping/stabilizing agent. In this study, we have demonstrated a rapid one-pot green route to fabricate monometallic (Ag and Au) and bimetallic NPs (Ag-Au) using the well-known bioactive flavonoid quercetin. The adopted synthesis protocol was facile, clean, and eco-friendly. At first, the Q-Ag, Q-Au, and Q-Ag-AuNPs synthesis were confirmed by the collective oscillations of electrons on NPs surface due to

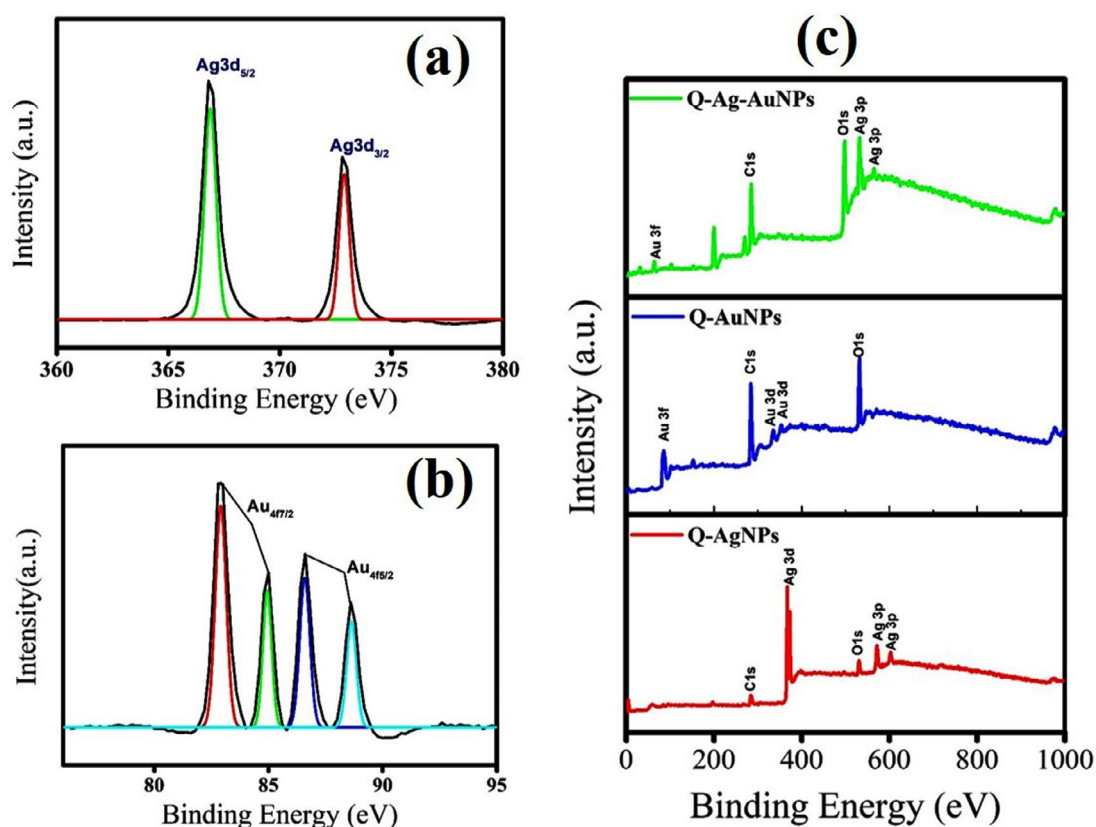


Figure 3. XPS analysis of fabricated NPs (a) Core level spectra of Q-AgNPs (b) core level spectra of Q-AuNPs (c) full scan spectra of all the three fabricated NPs.

the SPR effect. The SPR bands were recorded in UV-Vis spectrometer at 410, 530, and 420 nm for Q-Ag, Q-Au, and Q-Ag-AuNPs, respectively (Figure 1a-c). As per several earlier reports, biogenic preparations of mono and bimetallic NPs were largely influenced by reaction kinetics like temperature, the concentration of metal substrate, pH of the reaction medium, and contact time. Moreover, these reaction parameters play a pivotal role in controlling the size, shape, and dispersity of fabricated NPs. The UV-Vis spectra of Q-AgNPs and Q-AuNPs synthesized at various temperatures showed SPR spectrum variations. At lower reaction temperatures (60-70°C), the fabricated Q-AgNPs and Q-AuNPs generate a broad SPR peak with an absorption maximum at 423 and 536nm, respectively. The as-synthesized NPs at 90°C generate an intense sharp peak with a shift to lower wavelengths 405 and 524 nm (Figure 1a). The obtained results indicated that upon increasing

the reaction temperature, rapid nucleation growth of NPs occurs with narrow size distribution.¹⁹ Similarly, the slightly acidic pH 6.0 generates NPs with polydispersed in nature. Whereas the as-synthesized Q-AgNPs and Q-AuNPs at alkaline pH-9 produce very intense blue-shifted SPR peaks (Figure 1b), attributing to the enhanced ionization rate of Quercetin and metal ion reduction.²⁰ The concentration of metal ions such as Ag^+ and Au^{3+} is crucial for the fabrication of monodispersed NPs with less agglomeration. Our results showed that the NPs produced at 1 mM metal ion concentration possess intense SPR peaks at the lower wavelength region (Figure 1c), depicting that increasing the concentration resulted in larger particle formation.²¹ As shown in Figure 1d, the pure-Q shows at 3405 (O-H), 1658 (C=O), 1609-1560 (C=C), and 1380 (O-H in-plane bending of phenol), which substantially corroborated with a previous report.²² While the as-synthesized NPs mainly

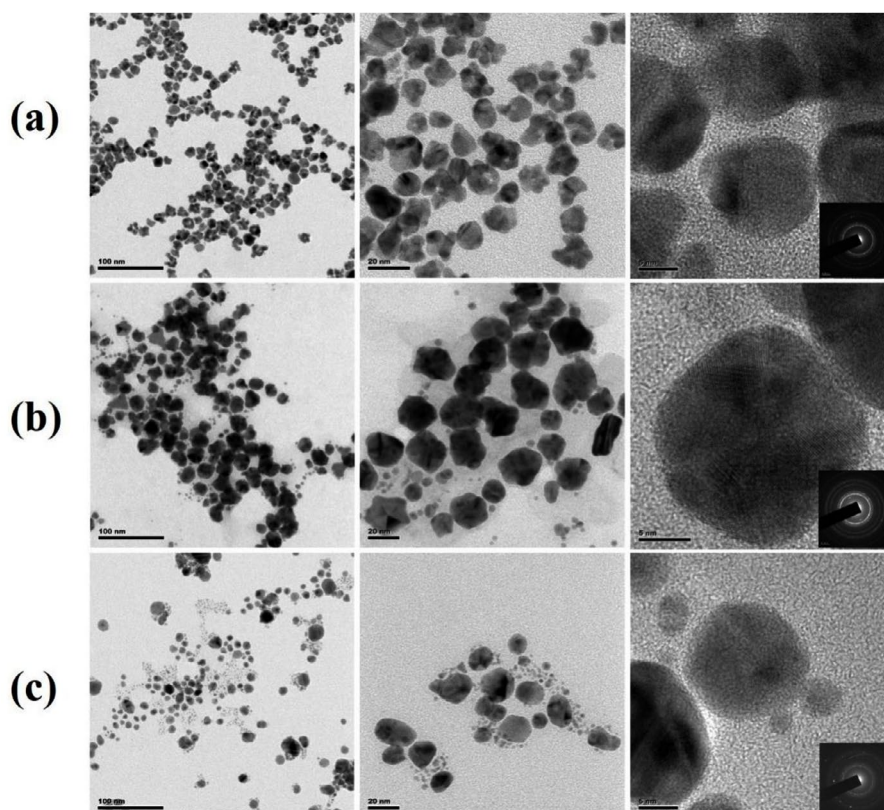


Figure 4.(i). HR-TEM micrographs of synthesized NPs (a) Q-AgNPs (b) Q-AuNPs, and (c) Q-A-AuNPs (inset the SEAD pattern of respective NPs).

show variations in the transmittance vibrations of hydroxyl (O-H) and carbonyl (C=O) functional groups manifesting their role in NPs formation.²³

From the DLS analysis and ζ -potential, the hydrodynamic diameter and colloidal stability of the noble metal NPs in an aqueous medium were determined. The hydrodynamic diameter of synthesized Q-Ag, Q-Au, and Q-Ag-AuNPs was 58.9, 96.02, and 141.6 nm, respectively. While the ζ -potential values are recorded as -22.9, -5.65, and -25.8, the synthesized bimetallic NPs are highly stable than individual mono-metallic NPs. The negative ζ -potential due to the presence of polyphenolic groups enforces a repulsive force among NPs, which ultimately leads to less accumulation and increased stability of NPs.²⁴ As given in Figure 2, the recorded XRD pattern of synthesized Q-AgNPs shows the peaks at 38.06°, 44.34°, 64.53° and 77.52° corresponding to [1 1 1],

[2 0 0], [2 2 0], and [3 1 1] planes of face-centered cubic crystalline structure of Ag (JCPDS file no 00-004-0783).²⁵ Likewise, the diffraction of planes of Q-AuNPs were noticed at 38.15°, 44.30°, 64.53° and 77.45° attributed to [1 1 1], [2 0 0], [2 2 0] and [3 1 1] planes of face-centered cubic structure of Au (JCPD file no 00-004-0784).²⁶ Our results proved that the biogenic Q-Ag, Q-Au, and Q-Ag-Au are having same lattice crystalline structure with increased stability.

XPS analysis determines the oxidation-state and chemical compositions of fabricated NPs. The deconvoluted high-resolution Ag 3d XPS spectra of Q-AgNPs ascertain Ag and AgO as major elements present in the sample. The binding energies of Ag 3d_{3/2} and Ag 3d_{5/2} at 367 and 372.9 correspond to Ag. As compared with the peak positions of Ag⁰ (368.3 eV and 374.3 eV), the peak shift to lower binding energies

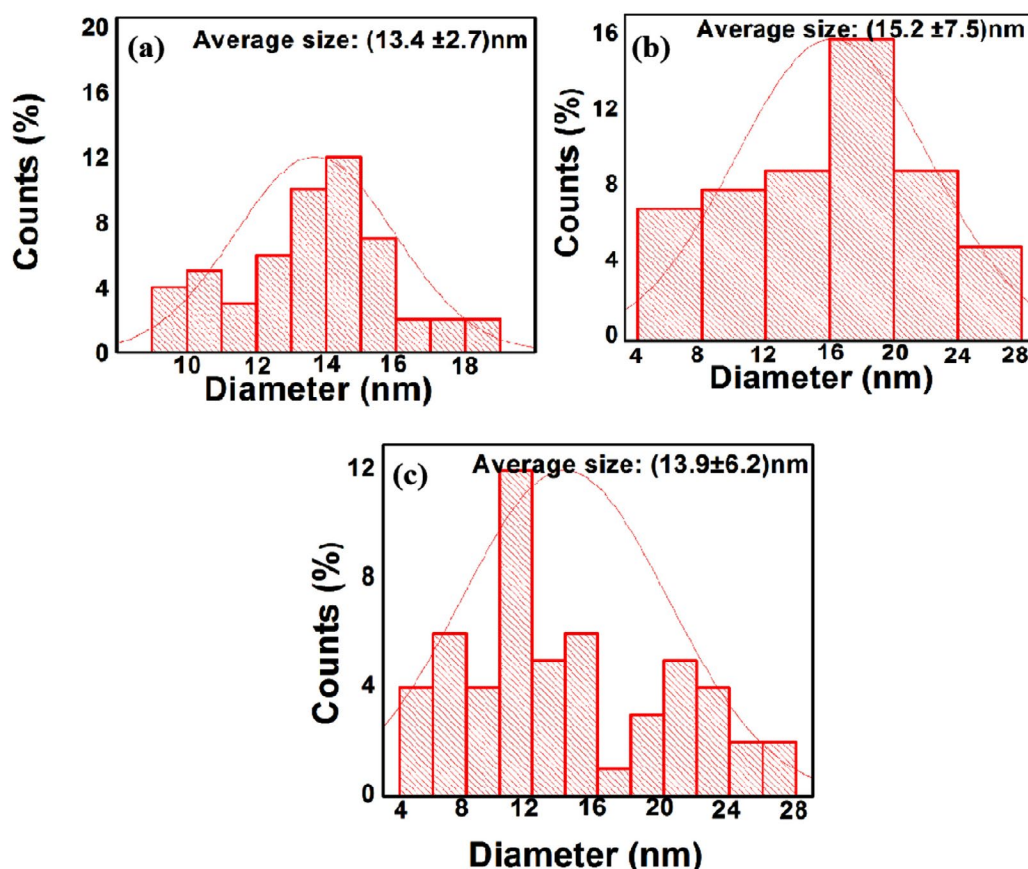


Figure 4. (ii). Histogram of particle size distribution for HR-TEM micrographs of synthesized NPs (a) Q-AgNPs (b) Q-AuNPs, and (c) Q-Ag-AuNPs.

attributes to the variation in the chemical nature of Ag atoms and flavonoid-Ag complex formation.²⁷ While, the high-resolution XPS spectra of Q-AuNPs show prominent peaks at 82.9 and 84.9, eV corresponding to Au 4f_{7/2}. Other peaks located at 86.6, and 88.6 correspond to 4f_{5/2}, the doublet peaks denote spin-orbit splitting and are consistent with earlier reported Au.²⁸ Further, the XPS survey spectra of Q-Ag, Q-Au, and Q-Ag-Au (Figure 3) indicate the chemical composition of C, O, and respective metals.

Figure 4(i) & (ii) a shows the HR-TEM micrographs of Q-AgNPs consisting of spherical, triangle, and trapezoid structures in size ranges between nm with an average size (mean value) of (13.4 ± 2.7) nm. The synthesized Q-AuNPs were spherical, triangle hexagonal, and trapezoid in shape with an average size (mean value) of (15.2 ± 7.5) nm [Figure 4(i) & (ii)b]. As shown in Figure 4(i) & (ii) c, the Q-Ag-AuNPs have a random distribution of NPs with various geometrical shapes around

the diameter (mean value) of (13.9 ± 6.2) nm. Higher magnification micrographs display the synthesized NPs with a Q-thin layer coating on their surface. Clear lattice fringes in the HR-TEM image and the typical SAED pattern with bright circular rings correspond to fcc planes, indicating that the synthesized MNPs are highly crystalline. These results are in agreement with XRD results.

In the well-diffusion assay, Q-AgNPs exhibited the highest level of inhibitory action, including *P. aeruginosa* (20±0.3), *Bacillus* sp. (20±0.6), and *P. vulgaris* (19±1.4). Whereas synthesized Q-Ag-AuNPs also show a significant bactericidal effect with the highest ZOI of *Bacillus* sp. (16±0.3), *K. pneumonia* (14±0.8), and *P. vulgaris* (14±0.8) (Table S1). It was explicitly observed that Q-AuNPs and pure-Q had exhibited only a moderate level of antibacterial effect against all the tested pathogens (Figure 5). All the fabricated NPs showed better antibacterial activity than pure-Q. Our earlier study proves the enhancement

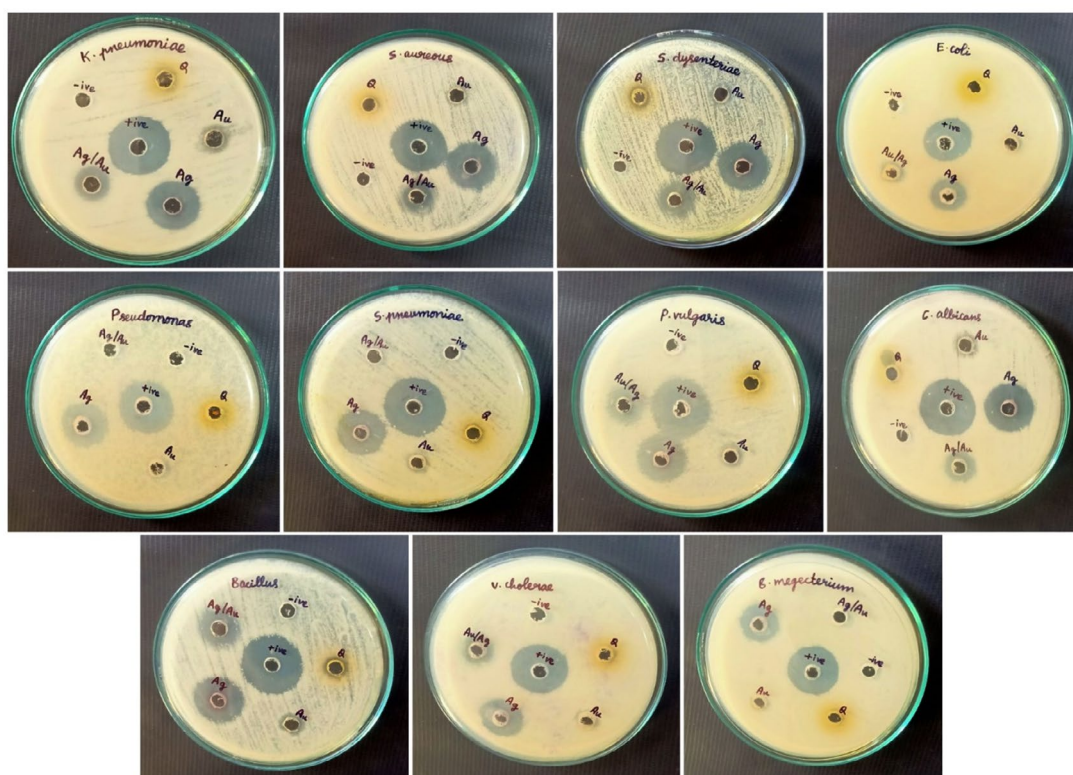


Figure 5. Antibacterial activity of synthesized NPs (Q-AgNPs, Q-AuNPs, Q-Ag-AuNPs, and pure-Q) against tested bacterial pathogens.

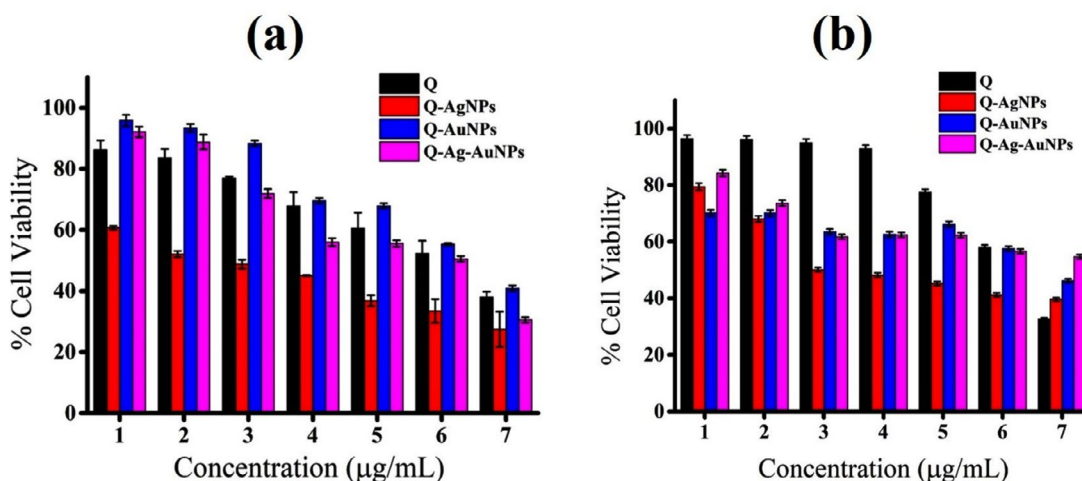


Figure 6. *In vitro* cell viability assay of synthesized NPs against (a) MCF-7 and (b) HCT-116 cancer cell lines after 48h treatment period. Values are mean \pm SD, n = 3, $p < 0.01$.

of natural flavonoids bactericidal effect after the complexation with metal NPs.²⁹ Recently, it was demonstrated that the biogenic Ag and AuNPs encrusted with citrus fruits flavonoids such as hesperidin (HDN) and Naringin (NRG) exhibited enhanced antibacterial action than the HDN and NRG alone.³⁰ The results confirmed that the synthesized NPs largely affect cellular permeability and membrane integrity, leading to cell death.³¹ It was reported that metal ions attach to the bacterial cell membrane, cause decomposition of cell membrane ingredients, and trigger plasmolysis.³² The size of NPs significantly influences the antibacterial effect, viz., small NPs with a large surface area can reach the cytoplasm more often than larger NPs.³³ After entering the cytoplasm, the NPs interact with cellular structures, sulfur-containing biomolecules (proteins & DNA), and lipids.³⁴ On the other hand, metal NPs also release the ions that trigger oxidative stress-mediated DNA damage and hinder the protein biosynthesis.³⁵

Cytotoxicity of both mono and bimetallic NPs was assessed against human breast and colorectal carcinoma cell lines (Figure 6). The cell viability percentage was reduced upon increasing the concentration of NPs and pure-Q from 1.56 to 100 $\mu\text{g/mL}$ with the incubation period of 48 h. In the MTT assay, the synthesized Q-AgNPs exhibit a higher level of cytotoxicity, followed by Q-Ag-AuNPs, pure-Q, and Q-AuNPs. At 100

$\mu\text{g/mL}$ concentration, all the treatments have shown more than 50% cytotoxic potential against MCF-7 and HCT-116 cell lines. In contrast, Yuan et al. reported that the flavonoid mediated graphene oxide (GO)-AgNPs composite possesses five-fold increased cytotoxicity against human neuroblastoma cancer cells (SH-SY5Y) mainly because of the high concentration loading of AgNPs onto GO surfaces.³⁶ It was also demonstrated that the Q-mediated bi-metallic NPs consisting of Ag exhibit increased anticancer efficacy.³⁷ According to the earlier studies, it was documented that MNPs functionalized with plant phenolics induce oxidative stress that leads to apoptosis via mitochondria-dependent and caspase-mediated pathways.³⁸⁻³⁹

CONCLUSION

To summarize, the reduction capabilities of pharmacologically active Quercetin were assessed. The surface chemistry of fabricating NPs indicated that the Ag and Au ions were entirely converted into elemental forms with a considerable display of Q-functionalization. In the application prospects, *in vitro* antibacterial properties of NPs unveiled that the fabricated NPs possess improved bactericidal effect against tested pathogens. As determined by MTT assay, the tested cancer cells lose their viability after the treatment with NPs. Based on the above studies,

biofunctionalized metal nanoformulations hold a bright future for therapeutic purposes. However, further studies were required on severe human pathogens and pre-clinical insights. As—synthesized metal NPs have excellent plasmonic properties, the future focus should be on diagnostic investigations to develop successful theranostic agents.

SUPPLEMENTARY INFORMATION

Supplementary information accompanies this article at <https://doi.org/10.22207/JPAM.16.3.03>

Additional file: Additional Table S1.

ACKNOWLEDGMENTS

The authors would like to thank Department of Science and Technology-Promotion of University Research and Scientific Excellence (DST-PURSE; DST Sanction Order No- SR/FT/LS-113/2009), Bharathidasan University, Trichy, India for providing instrument facility.

CONFLICT OF INTEREST

The authors declare that there is no conflict of interest.

AUTHORS' CONTRIBUTION

All authors listed have made a substantial, direct and intellectual contribution to the work, and approved it for publication.

FUNDING

None.

DATA AVAILABILITY

All datasets generated or analyzed during this study are included in the manuscript.

ETHICS STATEMENT

This article does not contain any studies with human participants or animals performed by any of the authors.

REFERENCES

1. Frieri M, Kumar K, Boutin A. Antibiotic resistance. *J Infect Public Health*. 2017;10(4):369-378. doi: 10.1016/j.jiph.2016.08.007
2. Cheng Z, Li M, Dey R, Chen Y. Nanomaterials for cancer therapy: current progress and perspectives. *J Hematol Oncol*. 2021;14(1):85. doi: 10.1186/s13045-021-01096-0
3. Panda MK, Dhal NK, Kumar M, Mishra PM, Behera RK. Green synthesis of silver nanoparticles and its potential effect on phytopathogens. *Materials Today: Proceedings*. 2021;35(2):233-238. doi: 10.1016/j.matpr.2020.05.188
4. Thanh NT, Green LA. Functionalisation of nanoparticles for biomedical applications. *nano today*. 2010;5(3):213-230. doi: 10.1016/j.nantod.2010.05.003
5. Pissuwan D, Valenzuela SM, Cortie MB. Therapeutic possibilities of plasmonically heated gold nanoparticles. *Trends Biotechnol*. 2006;24(2):62-67. doi: 10.1016/j.tibtech.2005.12.004
6. Li H, Yin D, Li W, Tang Q, Zou L, Peng Q. Polydopamine-based nanomaterials and their potentials in advanced drug delivery and therapy. *Colloids Surf B Biointerfaces*. 2021;199:111502. doi: 10.1016/j.colsurfb.2020.111502
7. Guo Q, Guo Q, Yuan J, Zeng J. Biosynthesis of gold nanoparticles using a kind of flavonol: Dihydromyricetin. *Colloids and Surfaces A: Physicochemical and Engineering Aspects*. 2014;441:127-132. doi: 10.1016/j.colsurfa.2013.08.067
8. Sathishkumar G, Bharti R, Jha PK, et al. Dietary flavone chrysin (5, 7-dihydroxyflavone ChR) functionalized highly-stable metal nanoformulations for improved anticancer applications. *RSC Advances*. 2015;5(109):89869-89878. doi: 10.1039/C5RA15060D
9. Xu LQ, Neoh KG, Kang ET. Natural polyphenols as versatile platforms for material engineering and surface functionalization. *Progress in Polymer Science*. 2018;87:165-196. doi: 10.1016/j.progpolymsci.2018.08.005
10. Zhou J, Lin Z, Ju Y, Rahim MA, Richardson JJ, Caruso F. Polyphenol-mediated assembly for particle engineering. *Acc Chem Res*. 2020;53(7):1269-1278. doi: 10.1021/acs.accounts.0c00150
11. Narayanan KB, Sakthivel N. Green synthesis of biogenic metal nanoparticles by terrestrial and aquatic phototrophic and heterotrophic eukaryotes and biocompatible agents. *Adv Colloid Interface Sci*. 2011;169(2):59-79. doi: 10.1016/j.cis.2011.08.004
12. Rajendran I, Dhandapani H, Anantanarayanan R, Rajaram R. Apigenin mediated gold nanoparticle synthesis and their anticancer effect on human epidermoid carcinoma (A431) cells. *RSC Advances*. 2015;5(63):51055-51066. doi: 10.1039/C5RA04303D
13. Azeem M, Hanif M, Mahmood K, Ameer N, Chughtai FRS, Abid U. An insight into anticancer, antioxidant, antimicrobial, antidiabetic and anti-inflammatory effects of Quercetin: a review. *Polymer Bulletin*. 2022;1-22. doi: 10.1007/s00289-022-04091-8
14. David AVA, Arulmoli R, Parasuraman S. Overviews of biological importance of Quercetin: A bioactive

- flavonoid. *Pharmacogn Rev.* 2016;10(20):84-89. doi: 10.4103/0973-7847.194044
15. Zhang Q, Zhao XH, Wang ZJ. Cytotoxicity of flavones and flavonols to a human esophageal squamous cell carcinoma cell line (KYSE-510) by induction of G2/M arrest and apoptosis. *Toxicology in Vitro.* 2009;23(5):797-807. doi: 10.1016/j.tiv.2009.04.007
16. Gibellini L, Pinti M, Nasi M, et al. Quercetin and cancer chemoprevention. *Evid Based Complement Alternat Med.* 2011;2011:591356. doi: 10.1093/ecam/nea053
17. Vimala R, Rajivgandhi G, Sridharan S, et al. Antimicrobial Activity of Extracellular Green-Synthesized Nanoparticles by Actinobacteria. *Methods in Actinobacteriology*, Springer. 2022a;717-720. doi: 10.1007/978-1-0716-1728-1_105
18. Vimala R, Rajivgandhi G, Sridharan S, et al. Cytotoxic Activity of Extracellular Green Synthesized Nanoparticles by Actinobacteria. *Methods in Actinobacteriology*, Springer. 2022;725-728. doi: 10.1007/978-1-0716-1728-1_107
19. Asimuddin M, Shaik MR, Adil SF, et al. Azadirachta indica based biosynthesis of silver nanoparticles and evaluation of their antibacterial and cytotoxic effects. *Journal of King Saud University-Science.* 2020;32(1):648-656. doi: 10.1016/j.jksus.2018.09.014
20. Nikaeen G, Yousefinejad S, Rahmdel S, Samari F, Mahdavinia S. Central composite design for optimizing the biosynthesis of silver nanoparticles using Plantago major extract and investigating antibacterial, antifungal and antioxidant activity. *Sci Rep.* 2020;10(1):1-16. doi: 10.1038/s41598-020-66357-3
21. Dubey SP, Lahtinen M, Sillanpaa M. Tansy fruit mediated greener synthesis of silver and gold nanoparticles. *Process Biochemistry.* 2010;45(7):1065-1071. doi: 10.1016/j.procbio.2010.03.024
22. Catauro M, Papale F, Bollino F, et al. Silica/quercetin sol-gel hybrids as antioxidant dental implant materials. *Sci Technol Adv Mater.* 2015;16(3):035001. doi: 10.1088/1468-6996/16/3/035001
23. Sathishkumar P, Li Z, Huang B, et al. Understanding the surface functionalization of myricetin-mediated gold nanoparticles: experimental and theoretical approaches. *Applied Surface Science.* 2019;493:634-644. doi: 10.1016/j.apsusc.2019.07.010
24. Adeyemi JO, Elemike EE, Onwudiwe DC, Singh M. Bio-inspired synthesis and cytotoxic evaluation of silver-gold bimetallic nanoparticles using Kei-Apple (*Dovyalis caffra*) fruits. *Inorganic Chemistry Communications.* 2019;109:107569. doi: 10.1016/j.inoche.2019.107569
25. Balachandran YL, Giriya S, Selvakumar R, Tongpim S, Gutleb AC, Suriyanarayanan S. Differently environment stable bio-silver nanoparticles: study on their optical enhancing and antibacterial properties. *PLoS One.* 2013;8(10):e77043. doi: 10.1371/journal.pone.0077043
26. Lomeli-Marroquin D, Cruz DM, Nieto-Arguello A, et al. Starch-mediated synthesis of mono-and bimetallic silver/gold nanoparticles as antimicrobial and anticancer agents. *Int J Nanomedicine.* 2019;14:2171. doi: 10.2147/IJN.S192757
27. Huang Z, Jiang H, Liu P, et al. Continuous synthesis of size-tunable silver nanoparticles by a green electrolysis method and multi-electrode design for high yield. *Journal of Materials Chemistry A.* 2015;3(5):1925-1929. doi: 10.1039/C4TA06782G
28. Deshmukh AR, Aloui H, Kim BS. Novel biogenic gold nanoparticles catalyzing multienzyme cascade reaction: glucose oxidase and peroxidase mimicking activity. *Chem Eng J.* 2021;421(2):127859. doi: 10.1016/j.cej.2020.127859
29. Gnanasekar S, Palanisamy P, Jha PK, et al. Natural Honeycomb Flavone Chrysin (5, 7-dihydroxyflavone)-Reduced Graphene Oxide Nanosheets Fabrication for Improved Bactericidal and Skin Regeneration. *ACS Sustain Chem Eng.* 2017;6(1):349-363. doi: 10.1021/acssuschemeng.7b02603
30. Anwar A, Masri A, Rao K, et al. Antimicrobial activities of green synthesized gums-stabilized nanoparticles loaded with flavonoids. *Sci Rep.* 2019;9(1):3122. doi: 10.1038/s41598-019-39528-0
31. Gopinath V, Priyadarshini S, Loke MF, et al. Biogenic synthesis, characterization of antibacterial silver nanoparticles and its cell cytotoxicity. *Arab J Chem.* 2017;10(8):1107-1117. doi: 10.1016/j.arabjc.2015.11.011
32. Abalkhil TA, Alharbi SA, Salmen SH, et al. Bactericidal activity of biosynthesized silver nanoparticles against human pathogenic bacteria. *Biotechnol Biotechnol Equip.* 2017;31(2):411-417. doi: 10.1080/13102818.2016.1267594
33. Raza M, Kanwal Z, Rauf A, Sabri AN, Riaz S, Naseem S. Size-and shape-dependent antibacterial studies of silver nanoparticles synthesized by wet chemical routes. *Nanomaterials.* 2016;6(4):74. doi: 10.3390/nano6040074
34. Ramalingam B, Parandhaman T, Das SK. Antibacterial effects of biosynthesized silver nanoparticles on surface ultrastructure and nanomechanical properties of gram-negative bacteria viz. *Escherichia coli* and *Pseudomonas aeruginosa*. *ACS Appl Mater Interfaces.* 2016;8(7):4963-4976. doi: 10.1021/acsami.6b00161
35. Mohamed MM, Fouad SA, Elshoky HA, Mohammed GM, Salaheldin TA. Antibacterial effect of gold nanoparticles against *Corynebacterium pseudotuberculosis*. *Int J Vet Sci Med.* 2017;5(1):23-29. doi: 10.1016/j.ijvsm.2017.02.003
36. Yuan YG, Wang YH, Xing HH, Gurunathan S. Quercetin-mediated synthesis of graphene oxide-silver nanoparticle nanocomposites: a suitable alternative nanotherapy for neuroblastoma. *Int J Nanomedicine.* 2017;12:5819-5839. doi: 10.2147/IJN.S140605
37. Mittal AK, Kumar S, Banerjee UC. Quercetin and gallic acid mediated synthesis of bimetallic (silver and selenium) nanoparticles and their antitumor and antimicrobial potential. *J Colloid Interface Sci.* 2014;431:194-199. doi: 10.1016/j.jcis.2014.06.030
38. Mukherjee S, Ghosh S, Das DK, et al. Gold-conjugated green tea nanoparticles for enhanced anti-tumor activities and hepatoprotection-Synthesis, characterization and *in vitro* evaluation. *J Nutr Biochem.* 2015;26(11):1283-1297. doi: 10.1016/j.jnutbio.2015.06.003